Materials Science & Engineering A 670 (2016) 75–80

Contents lists available at ScienceDirect

Materials Science & Engineering A

journal homepage: www.elsevier.com/locate/msea

# Study of spark plasma sintered nanostructured ferritic steel alloy with silicon carbide addition

Zhihao Hu, Kaijie Ning, Kathy Lu *

*Department of Materials Science and Engineering, Virginia Polytechnic Institute and State University, Blacksburg, VA 24061, USA*

ARTICLE INFO

*Article history:*
Received 13 April 2016
Received in revised form
31 May 2016
Accepted 1 June 2016
Available online 3 June 2016

*Keywords:*
Nanostructured ferritic alloy (NFA)
Silicon carbide (SiC)
Spark plasma sintering (SPS)
Density
Microstructure
Hardness

ABSTRACT

Pure nanostructured ferritic steel alloy (NFA) and NFA–silicon carbide (SiC) composites with different compositions (97.5 vol% NFA-2.5 vol% SiC and 95 vol% NFA-5 vol% SiC) have been sintered by spark plasma sintering (SPS) and systematically investigated based on XRD, SEM, density, Vickers hardness, and nano-hardness. Minor γ-Fe phase formation from the main α-Fe matrix occurs in pure NFA between the sintering temperature of 950 °C and 1000 °C. However, this is hindered in the NFA-SiC composite sintering. Densities for both the pure NFA and the NFA-SiC composites increase with the sintering temperature but decrease with the SiC content. The NFA-SiC composites have higher porosity than pure NFA under the same sintering condition. All the samples have the average grain sizes between 6 μm and 8 μm. Vickers hardness of the pure NFA and NFA-SiC composites is related to density and phase composition. By estimation, the 97.5 vol% NFA-2.5 vol% SiC composite sample has the maximum yield strength of $3.14 \pm 0.18$ GPa. Nano-hardness of the NFA-SiC composite is degraded by diffusion and reaction between NFA and SiC. The addition of SiC decreases the elastic modulus of the NFA-SiC composites.



## 1. Introduction

Cladding materials for nuclear fission and fusion energy systems are exposed to very high doses of neutron irradiation at high temperatures. These materials are required to maintain mechanical integrity over long term operation under such harsh environments [1–3]. Due to the excellent creep and irradiation resistances, nanostructured ferritic alloy (NFA) materials have been considered as a primary candidate for fission and fusion reactors [4]. The enriched nanoclusters and nanograined Fe-Cr alloy matrix of NFA materials [5–7] can enable mechanical enhancement and radiation resistance, for which traditional oxide dispersion strengthened (ODS) alloys are not able to achieve. The nanoclusters in the NFA alloys not only play the critical role of preventing dislocation gliding, grain growth, grain boundary slip, but also function as sinks to trap helium atoms and radiation-generated point defects. In addition, NFAs have excellent creep resistance, high temperature strength, and highly delayed radiation effects due to the prominent thermal stability of nanoclusters [4,7–11]. As a result, NFAs are desirable radiation shielding materials.

Silicon carbide (SiC) [12] is another structural material with high strength and chemical stability, especially in harsh environments. Even when exposed to radiation for a long time, SiC materials [13–15] still have low induced activation and low afterheat levels. SiC fiber-reinforced SiC-matrix composites ($SiC_f$/SiC) have prominent structural applications due to the enhanced mechanical properties and damage tolerance [16]. They are being considered as promising candidates for fuel cladding and channel boxes in light water reactors (LWR) and in-vessel components for advanced fission reactors [17–19].

Composite materials of NFA-SiC are expected to combine these advantages from each component. Such a composite would not only take advantage of the plastic deformation and energy absorption from the ductile NFA phase, but also provide the crack-propagation impedance for the highly brittle SiC. Meanwhile, the SiC component in the NFA-SiC composite would enhance high temperature stability that pure metallic structural materials cannot withstand and tolerate chemically harsh environments. As a result, the addition of SiC should reinforce the NFA matrix while the resistance to radiation is maintained.

In order to achieve high density for the NFA-SiC composites, spark plasma sintering (SPS) was used in this study. The SPS process relies on a pulsed direct current (DC) passing through an electrically conducting pressure die containing the green sample to densify the samples [20–23]. Full density can be reached relatively easily, and the entire process only takes a few minutes, thus minimizing the grain growth and any potential reactions.

In this work, density and microstructure evolution at different sintering temperatures were studied. The effects of a small amount of SiC addition on the sintering of the SiC-NFA composites were

* Corresponding author.
*E-mail address:* klu@vt.edu (K. Lu).

http://dx.doi.org/10.1016/j.msea.2016.06.003
0921-5093/

analyzed. Mechanical properties, such as Vickers hardness, nano-hardness, yield strength, and elastic modulus of the sintered samples, were investigated, and yield strength was derived from the hardness data.

## 2. Experimental procedures

### 2.1. Sample preparation and sintering

Commercial SiC particles (Grade UF-15, α-SiC, H.C. Starck, Karlsruhe, Germany) and lab-made NFA particles [4,7] were used as raw materials for pure NFA and NFA-SiC composite sintering. The NFA particles were screened with a mesh size of No. 653 (20 μm). Mean particle sizes for SiC and NFA were measured using a laser light scattering particle size analyzer (LA-950, HORIBA Scientific, Tenyamachi, Japan). The corresponding sizes were 1.24 μm and 14.28 μm, respectively. Ball-milling for the NFA and SiC powders was conducted in order to achieve homogeneous mixing. Then the powders were poured into a cylinder die, which had 20 mm diameter. The powder height was controlled at 5 mm. The densification process of the pure NFA and NFA-SiC composites was performed by spark plasma sintering (SPS Nanoceramics, Morton Grove, IL). Main sintering parameters included pressure (100 MPa), heating rate (50 °C/min), temperature (850 °C, 900 °C, 950 °C, 1000 °C), and holding time (10 min) for the pure NFA, 97.5 vol% NFA-2.5 vol% SiC, and 95 vol% NFA-5 vol% SiC samples.

### 2.2. Characterization

The density of the sintered samples was measured based on the Archimedes method. The phase composition was identified by X-ray diffraction (XRD, PANalytical B.V., Almelo, Netherlands). The microstructure was observed by scanning electron microscopy (FEI FEG-ESEM Quanta600, FEI Company, Hillsboro, OR, USA). Before the SEM observation, the sample surfaces were finely polished and ultrasonically cleaned. The elemental composition was measured by the energy-dispersive X-ray spectroscopy module (EDS, Bruker AXS, MiKroanalysis B.V., Gmbh, Berlin, Germany) attached to the SEM. The average grain sizes were measured from the ethanol-nitric acid etched surface. The statistical estimation for the average grain size was conducted for each sample with the grain number no less than 150. Vickers hardness was measured by using a macro-hardness tester (LV700AT, LECO, St. Joseph, MI). Fifteen indentations were performed for each sample with a load of 3 kg.

The Vickers hardness was calculated using the following formula [24,25]:

$$H_V = k\left(\frac{P}{d^2}\right) \quad (1)$$

where $k$ is the shape factor of the indenter, $P$ is the load to the indenter, $d$ is the diagonal length of the indention.

The yield strength was calculated using the following formula [26–28]:

$$\sigma_{YS} = \frac{1}{3}H_v \quad (2)$$

where $\sigma_{YS}$ is the yield strength, which has the unit of GPa.

The nano-hardness was measured by nano-indentation (TI 950 Triboindenter, Hysitron, Inc., Minneapolis, MN). A 100 nm 3-sided pyramidal diamond Berkovich tip was used during the measurement. A nano-indentation array of 15 indents was performed for each sample. The peak load was kept at 4000 μN for all the nano-indents. All the above measurements were conducted at room temperature.

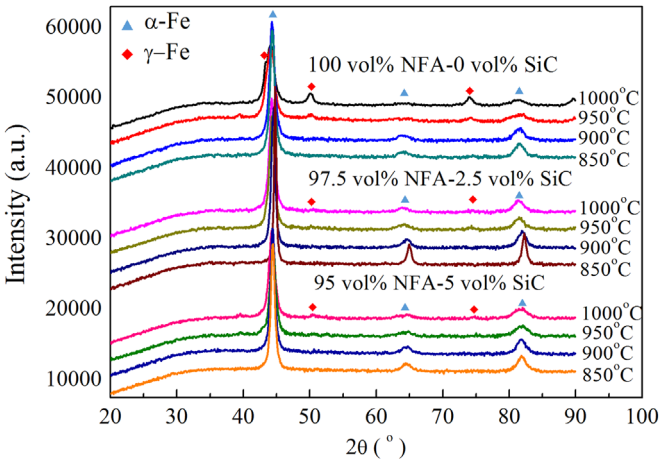


**Fig. 1.** XRD patterns of sintered pure NFA and NFA-SiC composite samples with different temperatures.

## 3. Results and discussion

### 3.1. Phase analysis

Fig. 1 shows the XRD patterns of the pure NFA, 97.5 vol% NFA-2.5 vol% SiC, and 95 vol% NFA-5 vol% SiC samples at different sintering conditions. All the samples show the well-crystallized α-Fe XRD patterns, and no SiC peaks can be observed. There are new peaks from $\gamma$-Fe at 950 °C and 1000 °C, while there are only peaks from $\alpha$-Fe at 850 °C and 900 °C. This is because the onset temperature of the α→γ Fe phase transformation is 948 °C [29]. In addition, the 100 vol% NFA sample after 1000 °C sintering gives the most obvious peaks from $\gamma$-Fe, while the 95 vol% NFA-5 vol% SiC and 97.5 vol% NFA-2.5 vol% SiC samples have only very small peaks from $\gamma$-Fe. This means that the addition of SiC delays the Fe $\alpha \rightarrow \gamma$ phase transformation and increases the phase transformation temperature.

Based on the Si-Fe phase diagram [30], when the atomic percent of Si is less than 3.8 at%, the phase transformation temperature increases with the increasing content of Si. In our system, the 95 vol% NFA-5 vol% SiC sample has 3.3 at% of Si. As a result, the phase transformation temperature increases from the 2.5 vol% SiC addition sample to the 5 vol% SiC addition sample. The fundamental process can be understood as follows. When sintering NFA-SiC composites, decomposition occurs and leads to the form of silicon and carbon at high temperatures [31–33]. It has been shown that the decomposition of SiC starts at 610 °C, then silicon diffuses into the lattice of iron to alloy with iron. The diffusion of silicon tends to de-stabilize γ-Fe and hinder the phase transformation of α-Fe→γ-Fe, raising the phase transformation temperature [34]. When the atomic percent of Si is above 3.8 at%, there is no phase transformation from $\alpha$-Fe to $\gamma$-Fe. Thus, the composites with SiC addition tend to have a much smaller content of $\gamma$-Fe. This explains why γ-Fe phase could hardly be observed in the 95 vol% NFA-5 vol% SiC composite sample even with sintering at 1000 °C.

### 3.2. Microstructure

Fig. 2 shows the SEM images of the sintered pure NFA and NFA-SiC composite samples. In Fig. 2(a–d), the microstructures of the pure NFA samples show that the sintered bodies are fairly dense without obvious pores. The NFA-SiC samples in Fig. 2(e–h) and Fig. 2(i–l), however, show different levels of porosity. The 97.5 vol% NFA-2.5 vol% SiC samples and 95 vol% NFA-5 vol% SiC samples have similar change tendencies in pore shape and porosity with the sintering temperature. For both of them, pores tend to become